THE JOURNAL OF BIOLOGICAL CHEMISTRY VOL. 284, NO. 19, pp. 13265–13276, May 8, 2009

Phosphorylation of Collapsin Response Mediator Protein 2 on Tyr-479 Regulates CXCL12-induced T Lymphocyte Migration*[S]

Received for publication, October 3, 2008, and in revised form, February 27, 2009 Published, JBC Papers in Press, March 10, 2009, DOI 10.1074/jbc.M807664200

Michel Varrin-Doyer, Peggy Vincent, Sylvie Cavagna, Nathalie Auvergnon, Nelly Noraz, Véronique Rogemond, Jérôme Honnorat, Mahnaz Moradi-Améli, and Pascale Giraudon[1]

From the Department of Neurooncology and Neuroinflammation, INSERM, U842, rue Guillaume Paradin, and UMR-S842, Université de Lyon, Lyon 1, Lyon 69372, France

In the central nervous system, collapsin response mediator protein 2 (CRMP2) is a transducer protein that supports the semaphorin-induced guidance of axons toward their cognate target. However, we previously showed that CRMP2 is also expressed in immune cells and plays a crucial role in T lymphocyte migration. Here we further investigated the molecular mechanisms underlying CRMP2 function in chemokine-directed T-cell motility. Examining Jurkat T-cells treated with the chemokine CXCL12, we found that 1) CXCL12 induces a dynamic re-localization of CRMP2 to uropod, the flexible structure of migrating lymphocyte, and increases its binding to the cytoskeletal protein vimentin; 2) CXCL12 decreases phosphorylation of the glycogen synthase kinase-3β-targeted residues CRMP2-Thr-509/514; and 3) tyrosine Tyr-479 is a new phosphorylation CRMP2 residue and a target for the Src-family kinase Yes. Moreover, phospho-Tyr-479 increased under CXCL12 signaling while phospho-Thr-509/514 decreased. The functional importance of this tyrosine phosphorylation was demonstrated by Y479F mutation that strongly reduced CXCL12-mediated T-cell polarization and motility as tested in a transmigration model and on neural tissue. We propose that differential phosphorylation by glycogen synthase kinase-3β and Yes modulates the contribution of CRMP2 to cytoskeletal reorganization during chemokine-directed T-cell migration. In addition to providing a novel mechanism for T lymphocyte motility, our findings reveal CRMP2 as a transducer of chemokine signaling.

T lymphocyte migration is the basis of major immune functions such as responses to infection and inflammation, as well as normal recirculation through the lymphoid organs. Indeed, the role of T-cells depends strongly on their ability to travel between organs via the blood and lymph and to move rapidly within these tissues, by extravasation (1). This latter function is dependent on extracellular signals, among which chemokines play a major role.

Chemokines form a superfamily of small proteins that orchestrate lymphocyte polarization and migration (2). These proteins exert their functions by binding specific seven-transmembrane-domain G-protein-coupled receptors on the T-cell surface (3). T-lymphocytes exposed to chemokines, in a soluble or surface-bound gradient, develop a polarized shape, extending at the front, an F-actin-rich lamellipodium, which constitutes the leading edge, and a trailing edge or uropod in which both the microtubule and vimentin networks are retracted during migration. Although F-actin has the well known function of producing the mechanical forces required to generate movement (4), the role of microtubules and vimentin in T-cell migration requires further investigation.

Cytoskeletal remodeling is of key importance in migrating cells (5) and is one of the functions carried out by the chemokine stromal cell-derived factor-1α, also named CXCL12. In association with its cognate receptor CXCR4, CXCL12 is a potent chemoattractant for mature T-cells and monocytes (6). Following ligand recognition and binding, CXCR4 signaling starts with the activation of G proteins, followed by various signaling cascade effectors, including MAP[2] kinases, phosphoinositide 3-kinase, and phospholipase Cγ (7). Although this intracellular signaling cascade has not been completely elucidated, the Src family non-receptor tyrosine kinase Lck and the Syk kinase ZAP-70 have emerged as the main candidates for delivering the input signal following CXCR4 activation (8). Thus, tyrosine kinase activity appears as a central step in CXCR4-dependent chemotaxis.

While searching for molecules involved in T-cell motility, we recently identified collapsin response mediator protein 2 (CRMP2) (9), a protein first described in the context of neuronal growth cone advance (10, 11). We demonstrated that CRMP2 regulated both T-cell polarization and spontaneous/chemokine-induced migration of T-lymphocytes. Moreover, CRMP2 was found at the uropod of motile T-cells and has the ability to bind cytoskeletal elements, including vimentin. A correlation between CRMP2 expression levels and cell migratory rates toward a chemokine gradient, including CXCL12, was

* This work was supported by grants and fellowships from the French Agency of Research on Multiple Sclerosis, INSERM, and Agence Nationale de la Recherche.

[S] The on-line version of this article (available at http://www.jbc.org) contains supplemental Figs. S1 and S2.

[1] To whom correspondence should be addressed: U842 INSERM, Faculty of Medicine R.Laennec, rue Guillaume Paradin, Lyon 69372, France. Tel.: 33-4-78-77-87-94; Fax: 33-4-78-77-86-16; E-mail: pascale.giraudon@inserm.fr.

[2] The abbreviations used are: MAP, mitogen-activated protein; Akt, v-akt murine thymoma viral oncogene homolog; CRMP2, collapsin response mediator protein 2; Cdk5, cyclin-dependent kinase 5; GSK-3, glycogen synthase kinase 3; Erk, extracellular signal-regulated kinase; DAPI, 4′,6-diamidino-2-phenylindole; GST, glutathione *S*-transferase; MOPS, 4-morpholinepropanesulfonic acid; C-ter, C-terminal; wt, wild type.

demonstrated by overexpression and knockdown experiments in T-cells (9). In addition, we recently reported that, in mouse model of neuroinflammation, elevated CRMP2 expression in T lymphocytes correlated with their elevated migratory rates and their ability to target the central nervous system (12). The importance of CXCL12 in the central nervous system and its implication in the pathogenesis of central nervous system disorders, including neuroinflammatory diseases, are well documented (review in Ref. 13). Thus, the aim of the present study was to determine whether and how CRMP2 participates in the transduction pathway induced by CXCL12 on T lymphocytes.

EXPERIMENTAL PROCEDURES

Cells and Antibodies—The Jurkat T-cell line was cultured in RPMI 1640 complemented with 10% fetal calf serum. Primary T lymphocytes selected from the blood of a healthy donor were cultured for 1–2 weeks in RPMI complemented with 10% AB human serum and interleukin-2 (20 units/ml).

Rabbit polyclonal antibodies recognizing both full-length and cleaved CRMP2 forms have been described previously (14). The peptide sequences used to generate C-ter and pep4 antisera were localized between amino acids 557–572 and 454–465 in the CRMP2 sequence, respectively. Antibodies were purified by affinity chromatography on the corresponding immobilized peptide. Sheep antisera recognizing CRMP2-pSer-522 (PB-044) and CRMP2-pThr-509/514 (PB-043) were from Kina Source Limited (Dundee, UK). Our rabbit polyclonal antibody was raised against a peptide phosphorylated on Tyr-479 (CRMP2-pTyr-479) and purified in a two steps method by affinity chromatography on the corresponding immobilized peptide (step 1: elimination of antibody anti un-phosphorylated peptide; step 2: purification of anti-phosphorylated peptide). Enzyme-linked immunosorbent assay performed against CRMP2-Tyr-479 and CRMP2-pTyr-479 peptides showed the specificity of our anti-CRMP2-pTyr-479 antibody. In addition, treatment of T-cell lysate with phosphatase calf intestinal phosphatase significantly reduced the positive signal of anti-pTyr-479 but not of anti-pep4 antibody analyzed in Western blot (supplement Fig. S1). Rabbit polyclonal antibody anti-Yes kinase (06.514) was from Upstate. Rabbit polyclonal antibody against the human phospho-Yes1-Y537 was from Abgent and showed cross-reaction with phospho-Src-Y530 a protein with very high homology. Mouse anti-vimentin (M0725) was from Dako. Anti-Erk (9102) and phospho-Erk (9101) antibodies from Cell Signaling Technology recognized the un-phospho- and phospho-p44/42 MAP kinase (Erk1 and Erk2). Anti-Cdk5 (SC-173), Cdk5-pTyr-15 (SC-12918), and Cdk5-pSer-159 (SC-12919) antibodies were from Santa Cruz Biotechnology. Rabbit anti-GSK-3β (AB8687) was from Chemicon International. Mouse anti-pGSK-3 from Upstate recognized the active forms of both GSK-3α (pTyr-279) and GSK-3β (pTyr-216) (05-413). Magnetic phospho enrichment beads (TALON® PMAC) were purchased from Clontech. Cell-permeable peptide inhibitor of GSK-3β, L803-mts, was from Calbiochem.

Plasmids and Constructs—The CRMP2-FLAG-wt plasmid has been described previously (14). Briefly, full-length CRMP2 was amplified by PCR and inserted directionally into the pCMV2-FLAG vector (Sigma). The mutation consisted of a two-step PCR procedure used to generate the CRMP2-Y479F mutant. First, a C-terminal fragment (471–572) containing the Y479F mutation was generated using a reverse primer introducing an EcoR1 site at the 3′-end and a forward primer with the codon: Tyr-479 (TAC) substituted with Phe (TTC). Next, this mutated fragment was used as a reverse primer in the second PCR reaction with a wild-type forward primer introducing a HindIII site at the 5′-end. The final PCR product was cloned into the HindIII and EcoRI sites of the pCMV2-FLAG vector, and the DNA sequence of the mutant was verified by sequencing. For the transfection, Jurkat T-cells were transfected with CRMP2-FLAG-wt, CRMP2-FLAG-Y479F, and empty-FLAG plasmids using Amaxa Nucleofector technology (Köln, Germany), according to the manufacturer's instructions. T-cells were used 18 h after transfection. Transfected cells were visualized by immunostaining with anti-FLAG antibody. The percentage of transfection reached 40–50% for most of the FLAG constructs.

Immunocytochemistry—The CRMP2 forms, Yes kinase and intermediary filament vimentin were detected by indirect immunofluorescence on Jurkat and primary T-cells adhered to collagen I-coated slides (20 μg/ml) and fixed following treatment (acetone −20 °C, 10 min). Cells were incubated with specific antibody (1 h, 37 °C) then with Alexa 488- or 546-conjugated anti-mouse or anti-rabbit or anti-sheep IgG antibodies (1 h, 37 °C) and examined using the Axioplan II fluorescence microscope (Carl Zeiss). Nuclear counterstaining was performed using a fluorescent DNA intercalant, 4′,6′-diamidino-2-phenylindole (DAPI, Roche Applied Science).

Protein Interaction Assay (Pulldown GST-CRMP2)—100 μl of Jurkat cell lysate, prepared as above, were added either to 80 μl of GST-CRMP2 protein fusion or to 80 μl of GST protein coupled with glutathione-Sepharose 4B (Amersham Biosciences, 1 h at 4 °C). GST-CRMP2 and GST beads were washed four times (50 mM Tris (pH 7.4), 1 mM EDTA, 150 mM NaCl, and 0.5% Nonidet P-40), and proteins bound to CRMP-2 or to GST beads alone were eluted. GST (in GST beads), Yes and CRMP2 (in GST-CRMP2 beads), and GST (in GST and GST-CRMP2 beads) were revealed by Western blotting.

Western Blotting—Following CXCL12 treatment, cells were lysed in homogenization buffer (Tris 20 mM, EDTA 1 mM, EGTA 5 mM, sucrose 10%, pH 7.4) complemented with phosphatase inhibitors (sodium fluoride (5 mM), sodium pyrophosphate (1 mM), β-glycerophosphate (1 mM), and orthovanadate (1 mM)) and with protease inhibitor mixture Complete™ (Roche Applied Science). Lysates were submitted to ultrasound to dissociate cell aggregates, and total proteins were measured by Lowry assay (Bio-Rad). Protein samples (10–20 μg) were subjected to SDS-PAGE under reducing conditions and transferred to a nitrocellulose membrane (BA85, Schleicher & Schuell Microscience) previously incubated with blocking solution (phosphate-buffered saline, 0.1% Tween 20, 5% nonfat dried milk, 1 h) and blotted against specific antibody (overnight, 4 °C), followed by incubation (1 h, room temperature) with rabbit and sheep IgGs antibody coupled with horseradish peroxidase and a chemiluminescence (ECL) detection system (Covalab, Lyon, France). Densitometric quantification of the immunoblot band was performed using ImageQuant (Molecu-

lar Dynamics), and the data were expressed as ratios to the amount detected before any treatment.

Data Base and Structure Analysis—The prediction program PROSITE was used to identify the putative tyrosine kinase site on CRMP2. The structure of CRMP2 was modeled, based on the coordinates available for CRMP2 chain D (15) (Protein Data Bank entry 2GSE), using Viewerlite/4.2 (Accelrys).

Cloning and Expression of CRMP2—The coding sequence for human CRMP-2 (NM_1386) was subcloned into the expression vector pEt21b (Novagen), resulting in a construct with an N-terminal hexahistidine tag. The plasmid was transformed into *Escherichia coli* BL21(DE3) cells. For expression, cells were grown in 1500 ml of Terrific Broth (containing 7% glycerol, 50 μg/ml kanamycin, and 100 μl of Breox®, Cognis) in bubble flasks. Cells were grown at +37 °C until an optical density of 2.5 at 600 nm was reached. The cultures were cooled to +18 °C for 1 h in a water bath. The expression of CRMP-2 was induced by the addition of 0.5 mM isopropyl 1-thio-β-D-galactopyranoside, and expression was allowed to continue overnight at +18 °C. Cells were harvested by centrifugation, and the pellets were suspended in lysis buffer (20 mM Tris, 500 mM NaCl, 1 mM dithiothreitol, 20% glycerol, 0.1% Triton, 10 mM imidazole) supplemented with Complete EDTA-free protease inhibitors (Roche Applied Science, Basel, Switzerland) and 2000 units of benzonase. The solution was sonicated for several cycles on ice. The samples were centrifuged at 14,000 × *g* for 30 min at 4 °C, and the supernatants were incubated with 1.5 ml of nickel-nitrilotriacetic acid resin 50% re-suspended in lysis buffer (Qiagen) at 4 °C for 90 min. His-tagged proteins were purified from nickel resin in a wash buffer (20 mM Tris, 500 mM NaCl, 1 mM dithiothreitol, 20% glycerol, 0.1% Triton, 20 mM imidazole) and were eluted with elution buffer (wash buffer plus 150 mM imidazole) in 1-ml fractions. Fractions were evaluated by SDS-PAGE.

Yes in Vitro Kinase Assay—Prior to the assay, His-tagged CRMP2 was dialyzed in buffer (40 mM MOPS, 0.5 mM EDTA, 5% glycerol) overnight at 4 °C using the Float-A-lyzer technology (Interchim), according to manufacturer instructions. For the Yes kinase assay, 0.6 μg of dialyzed His-tagged CRMP2 were incubated with 20 ng of recombinant full-length human Yes (Millipore) diluted beforehand in enzyme dilution buffer (20 mM MOPS, pH 7, 1 mM EDTA, 0.01% Brij, 0.1% β-mercaptoethanol, 5% glycerol). The reaction was allowed in 50 μl of reaction buffer (8 mM MOPS, 0.2 mM EDTA, 30 mM $MgCl_2$, 2 mM EGTA, 10 mM β-glycerophosphate, 0.4 mM Na_3VO_4, 0.4 mM dithiothreitol, 200 μM ATP) at 30 °C for 10 min. The reaction was stopped with loading buffer, and the mixture was resolved on SDS-PAGE gels.

Transmigration Assay—T-cell transmigration was performed with Jurkat T-cells both in micro-Transwell systems (Costar Transwell Supports, A) and in organotypic cultures of mouse brain (B). A: Transmigration was performed in triplicate in Transwell systems (Boyden chamber, Costar, 5-μm diameter pore size membrane), as described previously (9). Briefly, the T-cell preparation (3×10^5 cells/well) was added in the upper chambers and CXCL12 in the lower compartment (10 ng/ml). Following a 2-h incubation at 37 °C, cells migrating in the lower chambers were counted under the microscope (at least 30 fields examined). B: T-cell transmigration on neural tissue was assayed on hippocampal cultures prepared as follows. Hippocampi from postnatal (P7) C57BL6 mice were dissected and placed immediately in cold Gey's balanced solution supplemented with glucose (6.5 mg/ml). 400-μm slices were cut perpendicularly to the septotemporal axis of the hippocampus using a McIllwain tissue chopper. Slices were carefully trimmed for excess tissue, and 6 slices were placed immediately on 30-mm semi-permeable membrane inserts (Millicell-CM, Millipore) in a 6-well plate, each well containing 1 ml of culture medium. The culture medium consisted of 50% minimum essential medium (Invitrogen), 25% Hanks balanced salt solution, 25% heat-inactivated horse serum (Invitrogen), 1% l-glutamine 200 Mm (Invitrogen), and 6.5 mg/ml D-glucose. Plates were incubated at 37 °C and 5% CO_2. The culture medium was exchanged twice a week. Jurkat T-cells (1×10^6 cells per slice) stained *ex vivo* using the vital fluorochrome carboxyfluorescein succinimidyl ester (1 mM, 5 min, 37 °C) were spotted close to the hippocampus slices (3 week culture). Following 18 h contact at 37 °C, slices were extensively washed with D-MEM, fixed with ethanol (10 min, 4 °C), and incubated with DAPI for nuclear counterstaining.

Statistical Analysis—Statistical significance in comparing two means was tested with the unpaired Student's *t* test; *p* values < 0.05 were considered significant. In the migration test, the number of migratory lymphocytes was counted by light microscopy (15–20 microscope fields per condition with 2 or 3 independent experiments), and data were expressed as the mean number of migratory lymphocytes per field.

RESULTS

CXCL12 Induces CRMP2 Polarization at the T Lymphocyte Uropod—To define a link between chemokines and CRMP2, we first examined the localization of CRMP2 in Jurkat T-cells under CXCL12 signaling. We used two different anti-CRMP2 antibodies (anti-C-ter and anti-pep4) that recognize the full-length and cleaved products of CRMP2. An immunofluorescence study of untreated T-cells revealed that CRMP2 was found within the T-cell cytoplasm as *punctate dots* (Fig. 1*A*, *0mn*). Under CXCL12 treatment, CRMP2 moved to the cell trailing edge within 2 min and showed quasi-exclusive uropod localization in most polarized cells after 10-min treatment (Fig. 1*A*, anti-C-ter antibody). This phenomenon of CRMP2 polarization was still observed after 30 min of treatment (not shown). Un-treated Jurkat T-cells showed an asymmetrical CRMP2 distribution in cells, but increases of 1.6- to 2-fold were observed after CXCL12 treatment (Fig. 1*A*, *graph*). Similar CRMP2 re-localization was observed with anti-pep4 antibody staining (not shown). In addition CRMP2 distribution to the uropod was concomitant with the re-localization of vimentin, which was quickly redistributed at the trailing edge of polarizing T-cells (Fig. 1*B*, *right panel*). Interestingly, CRMP2 re-localization was reversed to a great extent (35% decrease) in the presence of AMD3100, an antagonist of the CXCL12 receptor (CXCR4), consequently confirming the specificity of the CXCL12-induced response (Fig. 1*C*). These results supported the idea that chemokines can induce a dynamic re-localization of CRMP2 in

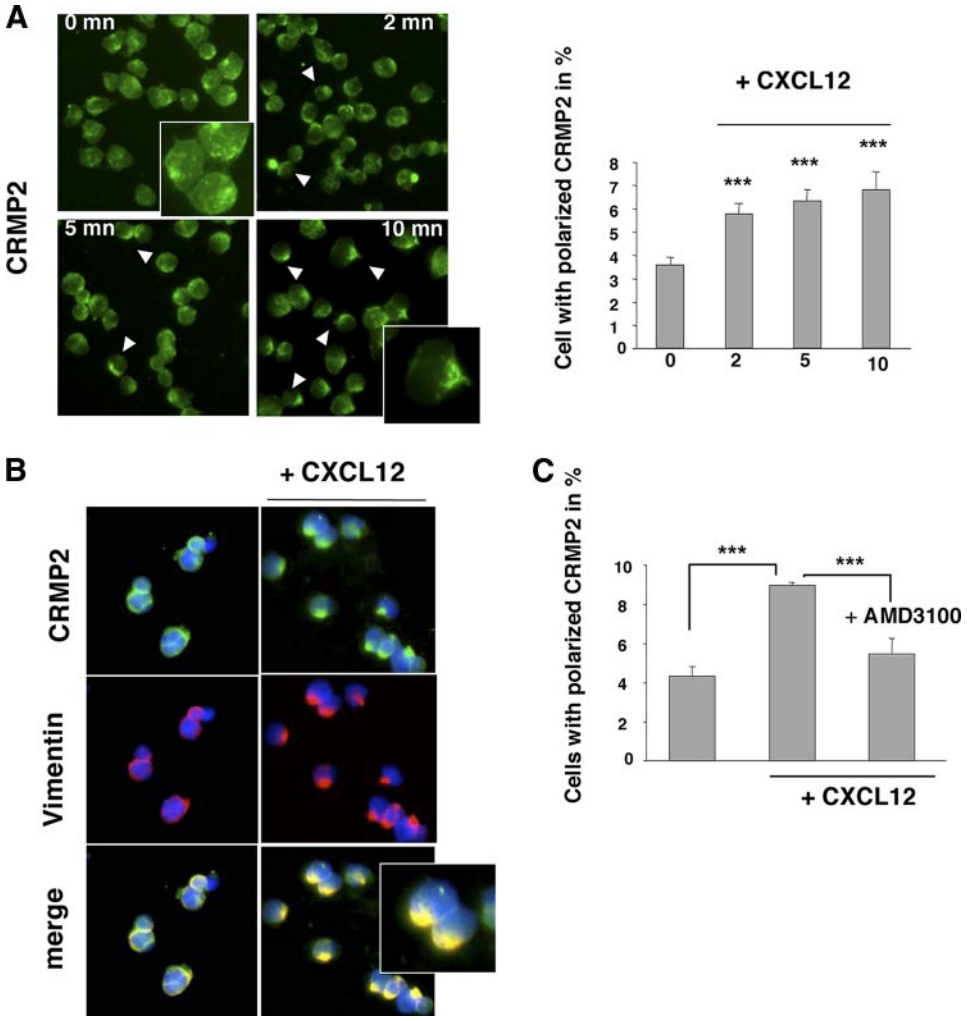

FIGURE 1. **CXCL12 induced a polar distribution of CRMP2 at the T-cell uropod.** Jurkat T-cells were allowed to adhere to collagen 1-coated slides, treated with CXCL12 (100 ng/ml), and examined for CRMP2 distribution at 0, 2, 5, and 10 min post-treatment following fixation. *A*, immunostaining with anti-CRMP2-C-ter antibody (*left panel*) showed a markedly elevated number of cells with polarized CRMP2 (*graphical representation*) under CXCL12 treatment. *B*, co-distribution of immunodetected CRMP2 and vimentin at the uropod in CXCL12-treated T-cells. Nuclei stained blue by DAPI (CRMP2 staining using two different specific antibodies). *C*, treatment of Jurkat T-cells with the CXCR4 antagonist AMD3100 specifically reduced the number of cells exhibiting polarized CRMP2 under CXCL12 treatment, confirming the association between CXCL12 signaling and CRMP2.

T lymphocytes in concert with vimentin, namely in the flexible uropod structure.

CXCL12 Modulates CRMP2 Binding to the Cytoskeleton—It is well known that T-cell uropods are rich in vimentin and microtubules (5), two cytoskeletal elements that have both been described as CRMP2 binding partners (9, 16) and actors in T-lymphocyte polarization and migration (17). This led us to hypothesize that CXCL12 could modulate CRMP2 binding to the cytoskeleton to promote T-cell motility. Following CXCL12 treatment (100 ng/ml, 10 and 30 min), subcellular fractionation was performed on Jurkat T-cell extracts to isolate cytoskeletal elements and associated proteins from the cytosol fraction. Identification of the subcellular fractions using antibodies against vimentin, tubulin poly(ADP-ribose) polymerase, and Hsp90 indicated that there was no contamination between cytoskeletal and cytosolic fractions (not shown). The cytoskeletal fraction displayed the intermediate filament vimentin but was free from tubulin, probably due to de-polymerization as it is found in the cytosol (not shown). Different fractions were then subjected to Western blotting using anti-CRMP2 antibodies. In whole cell lysates of untreated cells, anti-C-ter antibody revealed CRMP2 bands corresponding to the previously described full-length CRMP2 (62 kDa) and bands with higher molecular mass (Fig. 2*A*). Anti-pep4 antibody mainly recognized a 58-kDa band, corresponding to the cleaved form of CRMP2, as reported in neural cells (14). After CXCL12 treatment, the efficiency of which was assessed by Erk1/2 phosphorylation (Fig. 2*A*), no difference in CRMP2 expression was detectable in whole cell lysates. However, the distribution of CRMP2 forms differed according to the T-cell compartment examined. Full-length CRMP2 and higher molecular weight bands were found in the cytosolic fractions. These did not show major alterations under CXCL12 treatment. CRMP2 was also found, to a lesser extent, in the cytoskeletal fractions as 62-kDa full-length and 58-kDa cleaved forms. Interestingly, the expression of both forms was enhanced following CXCL12 treatment. It should be noted that the majority of cleaved CRMP2 was found in the nucleus (not shown), as previously reported in neural cells (14) and was not modified under CXCR4 activation. These results showed that CRMP2 was distributed in the cytoskeletal compartment of T lymphocytes and that CXCL12 had the ability to alter this distribution, enhancing CRMP2 association with cytoskeletal elements.

CXCL12 Increases CRMP2 Phosphorylation—Functional regulation of CRMP2 in neural cells is mainly dependent on its phosphorylation state, notably via GSK-3β and Cdk5 kinase activity (18). We therefore asked whether, in T lymphocytes, CXCL12 could modify CRMP2 binding to the cytoskeleton through modulation of its phosphorylation. To evaluate CRMP2 phosphorylation, we performed a phosphoprotein-enrichment assay (TALON® PMAC, Clontech) on whole cell extracts of Jurkat T-cells following CXCL12 treatment (100 ng/ml) and carried out immunoblotting on the non-phosphorylated (flow through) and phosphorylated (eluate) fractions by Western blotting at 2, 5, 10, and 30 min post-treatment. The full-length CRMP2 forms revealed by the anti-C-ter antibody were present in both the un-phosphorylated and phosphorylated fractions (Fig. 2*B*). In contrast, the cleaved form of CRMP2

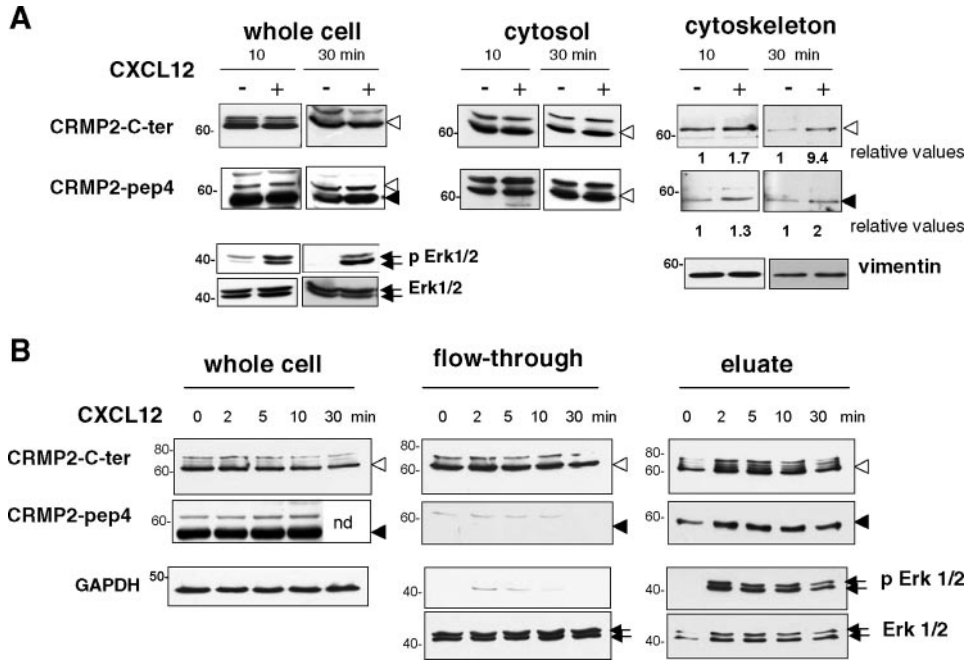

FIGURE 2. **CXCL12 promoted CRMP2 association with the cytoskeleton and enhanced CRMP2 phosphorylation.** *A*, Jurkat cells were treated with CXCL12 (100 ng/ml, 10 and 30 min), and cell lysates were subjected to subcellular fractionation, then Western blotting using anti-CRMP2-pep4 and -C-ter antibodies. Full-length (*open arrow*) and cleaved (*black arrow*) CRMP2 forms were detected in the cytoskeletal fraction (identified by vimentin detection), and increased under CXCL12 treatment (see relative values). The full-length forms distributed in the cytosol did not show major modification. CXCR4 activation was assessed by increase in phospho-Erk1/2 products (representative experiment from three different experiments). *B*, Jurkat T-cells were treated with CXCL12 (100 ng/ml), and cell lysates were subjected to phosphorylated form enrichment at 0, 2, 5, 10, and 30 min post-treatment. Whole cell extract, unphosphorylated (flow through) and phosphorylated proteins (eluate, authenticated by phospho-Erk1/2 detection) were Western blotted using CRMP2 antibodies. Full-length forms (*open arrow*) distributed in both phospho- and unphosphorylated fractions, while the cleaved form of CRMP2 (*black arrow*) was found mainly in the phosphorylated pool. Phosphorylated CRMP2 increased under CXCL12 treatment. CXCR4 activation was assessed by the induction of phospho-Erk1/2 products.

was only found in the phosphorylated protein pool, indicating that this form is mostly phosphorylated. CXCL12 treatment rapidly increased the level of CRMP2 phosphorylated forms, peaking at 2 min post treatment and still high at 30 min. The efficiency of the phosphoprotein-enrichment procedure was ascertained by phospho-Erk1/2 immunoblotting, which confirmed the specific presence of phosphorylated proteins in the eluate and at the same time, the increase following CXCL12 treatment. Similar experiments performed on primary T-lymphocytes isolated from healthy donors showed similar observations (not shown). A more precise evaluation of CRMP2 phosphorylation in response to CXCL12 was carried out using anti-CRMP2-pSer-522 and anti-CRMP2-pThr-509/514 antibodies recognizing two sites targeted by Cdk5 and GSK-3 kinases, respectively (Fig. 3*A*). Immunoblotting of Jurkat cell lysates showed that CRMP2-pSer-522 and CRMP2-pThr-509/514 were present as full-length 62-kDa CRMP2 in T-cells and were variously expressed during chemokine treatment, the efficiency of which was ascertained by phospho-Erk1/2 detection. Although Ser-522 phosphorylation was found at relatively low levels, Thr-509/514 phosphorylation decreased quickly by 4 min and was undetectable thereafter. This was consistent with the activity of Cdk5 and GSK-3 kinases evaluated by the detection of Cdk5-pTyr-15, Cdk5-pSer-159, GSK-3α-pTyr-279, and GSK-3β-pTyr-216, the active forms of these kinases (Fig. 3*B*). Cdk5 displayed a stable level of phosphorylation on Tyr-15 and Ser-159, reflecting a conserved level of Cdk5 activation. In contrast, GSK-3 exhibited de-phosphorylation mainly detected on the GSK-3β isoform, revealing a decreased activity starting at 4 min post-treatment. Taken together, these results first revealed, as previously described in neural cells, that the CRMP2 residues Ser-522 and Thr-509/514 could be phosphorylated in T lymphocytes. More importantly, they demonstrate that CXCL12 triggers a signaling cascade leading to differential modulation of CRMP2 phosphorylation of these residues, namely with a net decreased phosphorylation on Thr-509/514. Intriguingly, these modulations were mainly detected on the full-length CRMP2 forms, whereas phosphoprotein-enrichment assays (Fig. 2*B*) showed a strong phosphorylation of the cleaved CRMP2 form following chemokine treatment. This led us to suspect the participation of an additional phosphorylated target in the response of CRMP2 to CXCL12.

Tyrosine 479 Is a New Phosphorylation Residue in CRMP2 Sequence—It is known that CXCL12 triggers a tyrosine phosphorylation cascade in T-lymphocytes, which involves the serial recruitment and activation of tyrosine kinases, including Lck, ZAP-70, and Itk (8). We therefore searched for tyrosine target residues potentially modulated under chemokine treatment by analyzing CRMP2 protein sequences. A data base study of the 572 amino acids identified tyrosine 479 (Tyr-479) as a potential new phosphorylation residue, located in the phosphotyrosine consensus motif K*XXX*D*XX*Y within residues 472–479 (Fig. 4*A*). In addition, inspection of this region also showed the presence, close to Tyr-479, of a putative SH3-binding motif of the form R*XX*-P*XX*P within residues 467–473. To assess the accessibility of these sequences to binding protein partners, we evaluated the position of both Tyr-479 and the SH3-binding motif within the known structure of CRMP2 (Fig. 4*A*) based on the coordinates available for fragment 15–489 (15). Surface exposure representation of this CRMP2 form revealed that, in contrast to Tyr-479, the putative SH3-binding motif was exposed, suggesting a possible binding with SH3-domain bearing proteins (Fig. 4*A*, *inset*). It has been shown that interaction with the SH3 domain-binding motif induces protein conformational changes (19), so the latter could be the basis of subsequent Tyr-479 exposure. These observations suggested Tyr-479 as a major putative phosphorylation tyrosine within the CRMP2 sequence.

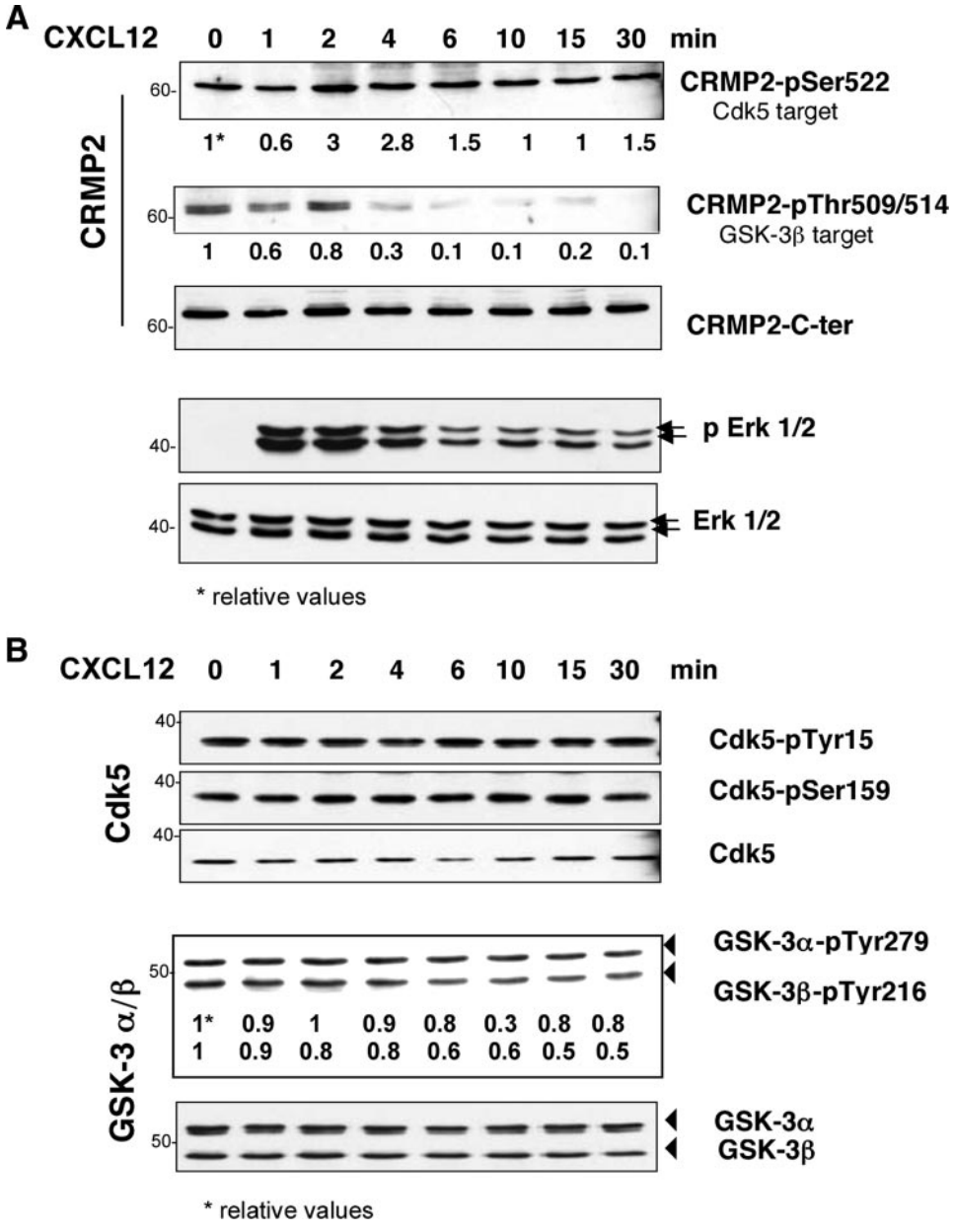

FIGURE 3. **CXCL12 differentially modulated CRMP2 phosphorylation on Cdk5 and GSK-3 target residues.** *A*, Jurkat T-cells were treated with CXCL12 (100 ng/ml, 0, 1, 2, 4, 6, 10, 15, and 30 min). Cell lysate blotting against anti-C-ter CRMP2 and the forms phosphorylated on Ser-522 and Thr-509/514, targets of Cdk5 and GSK-3β kinases, respectively, showed a decrease in CRMP2- pThr-509/514 under CXCL12 treatment, which was assessed by the induction of phospho-Erk1/2 products. *B*, blotting against the kinases Cdk5 and GSK-3 and against their active forms Cdk5-pTyr-15, Cdk5-pSer-159, GSK-3α-pTyr-279, and GSK-3β-pTyr-276 showed the presence and activity of GSK-3 and Cdk5. CXCL12 induced a progressive decrease in GSK-3β-pTyr-276 (see relative values).

CRMP2 Tyrosine Phosphorylation Is Carried Out by the Src-family Kinase Yes and Increases under Chemokine Treatment—In view of the presence of the putative SH3-binding motif close to the potential phosphorylatable site Tyr-479, a possible interaction between CRMP2 and tyrosine kinases through its SH3 domain was studied. This was done using a membrane array bearing several protein SH3 domains that remain folded in active conformations. Ten different lymphocyte tyrosine kinases, including Abelson kinase (Abl), Src family kinases (Lck, Yes, c-Src, Fyn, Hck, and Blk), and Tec family kinases (Itk, Txk, and Btk) were present in this array. Following His-tagged recombinant CRMP2 hybridization, protein-protein interactions were visualized using anti-His antibody, and spot intensities revealed the interaction strength (Table 1). Yes kinase displayed a strong binding to CRMP2, whereas Blk and Abl showed weak signals. In addition, four non-kinase protein SH3-domains belonging to Vav1, phospholipase Cγ, ITSN, and PI3β also displayed strong binding to CRMP2. Interestingly, phospholipase Cγ and ITSN have previously been observed as binding partners for CRMP2 (20, 21). We then focused on Yes, the more potent tyrosine kinase candidate for CRMP2 phosphorylation.

The Yes/CRMP2 interaction was evaluated by several approaches. First, localization of these proteins was assessed on primary T lymphocytes and Jurkat T-cells that had been allowed to adhere onto collagen-I-coated coverslips and then treated with CXCL12 (100 ng/ml, 5 min) (Fig. 4*B*). Immunofluorescence, performed with anti-Yes and anti-pep4 antibodies, showed the co-distribution of CRMP2 and Yes, especially at the uropod of polarized T-cells. Yes-CRMP2 interactions were next examined by a GST pull-down assay using cell lysates from primary T-lymphocytes and from neural cells (Dev cell line) (Fig. 4*C*), because CRMP2 is also involved in motility in the central nervous system. CRMP2 immobilized on glutathione-Sepharose beads was incubated with cell lysates. Western blots, performed on eluates from both cell types, showed the presence of Yes protein in association with CRMP2-GST, but not with GST alone. Taken together, these results defined the Yes kinase as a potent binding partner for CRMP2. To evaluate the functional significance of this interaction, an *in vitro* kinase assay was performed using active recombinant human Yes kinase and His-tagged CRMP2 as a substrate (Fig. 4*D*). Phosphorylation was detected using an anti-phospho-Tyrosine antibody by immunoblotting. A control was carried out in the absence of CRMP2, which showed Yes self-phosphorylation. A band corresponding to CRMP2 phosphorylation was detected only in the presence of ATP. As a consequence of protein phosphorylation, this band displayed a slight increase in molecular weight.

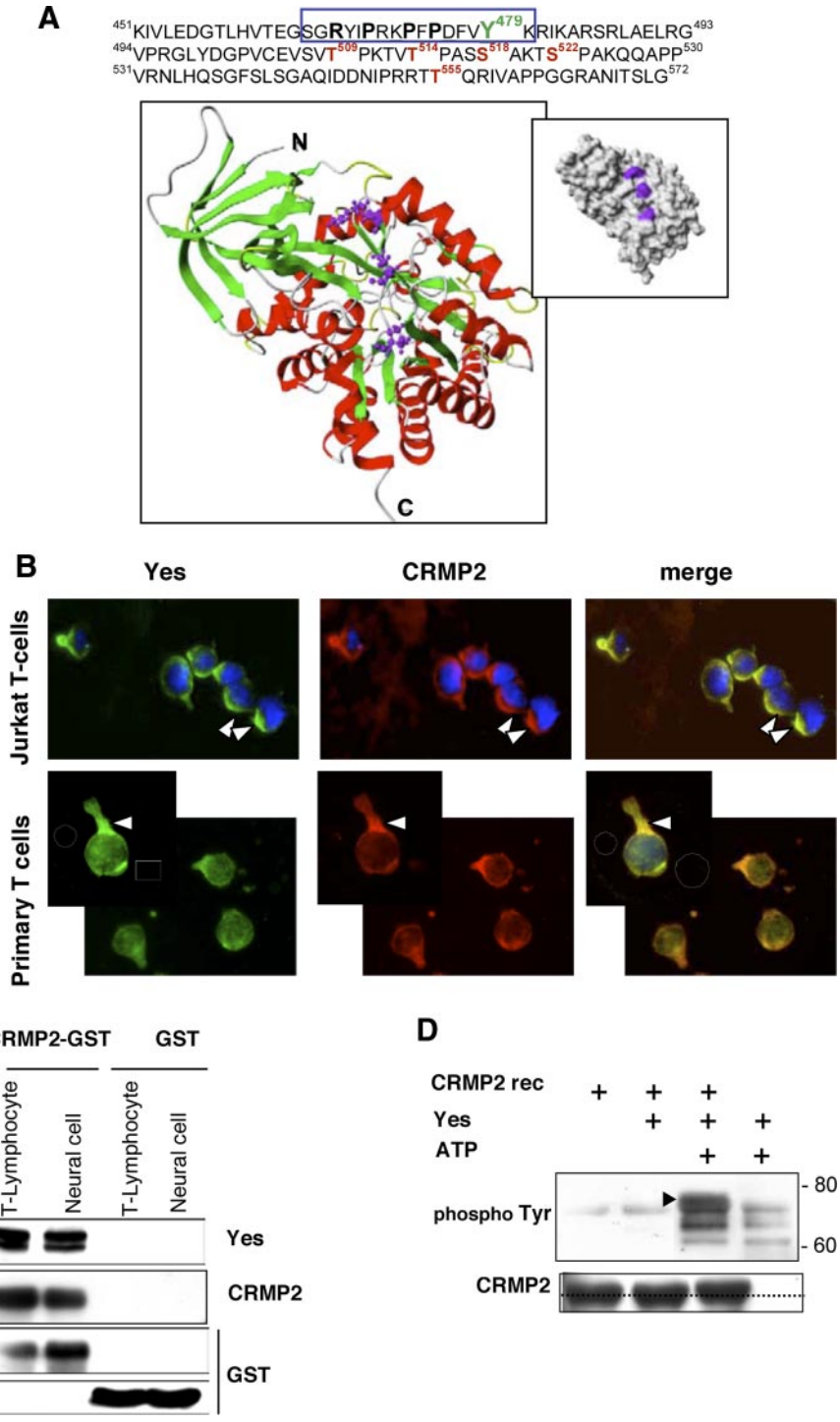

FIGURE 4. **Yes of the Src family is a tyrosine kinase partner for CRMP2.** *A*, identification of a potential tyrosine phosphorylation residue, Tyr-479, in the phosphotyrosine consensus motif K*XXXDXXY* (amino acids 472–479) on CRMP2, close to a putative SH3-binding motif (R*XXP*P*XX*P). The surface exposure of the SH3 binding motif in the CRMP2 structure is shown in a *ribbon diagram* revealing the structure of short CRMP2 from residues 15 to 489. The helices are distinguished by their *red color*, the strands are in *green*, and the turns are in *white*. The putative SH3 binding domain involves residues Arg-467, Pro-470, and Pro-473, shown as *ball-and-stick representations*. These residues are located in a flexible part N-terminal to the last α helix. The *inset* shows the surface representation of short CRMP2, indicating the surface exposure of residues Arg-467, Pro-470, and Pro-473 (*magenta*). *B*, co-detection of Yes and CRMP2 in primary T-cells and the Jurkat T-cell line allowed to adhere to collagen I-coated slides, then treated with CXCL12 (100 ng/ml, 15 min, *orange* as *merge color*). *C*, protein interaction assay (GST pulldown): Sepharose-4B beads coupled to the fusion protein CRMP2-GST and GST were added to the cell lysates of primary T lymphocytes and Dev neural cells. Blotting eluates against Yes, CRMP2, and GST validated the binding of Yes with CRMP2-GST beads and not with GST alone. *D*, *in vitro* kinase assay was performed with active recombinant Yes (Millipore), and recombinant CRMP2 protein Western blotting against phospho-Tyr residues detected CRMP2 phosphorylation on tyrosine in the presence, but not in the absence, of ATP. Blotting to CRMP2 detected a slight increase in molecular weight following CRMP2 phosphorylation.

To confirm the presence of tyrosine-phosphorylated forms of CRMP2 in T-cells, a polyclonal antibody was raised against a fragment of the CRMP2 sequence containing the phosphorylated residue Tyr-479. Immunoblotting with this antibody revealed the presence of CRMP2-pTyr-479 in T-lymphocytes, detected as both full-length and 58-kDa cleaved proteins. Examination of CRMP2-pTyr-479 in Jurkat T-cells treated with CXCL12 (100 ng/ml; 0, 2, 5, 8, 14, 20, and 30 min) showed an increase in Tyr-479 phosphorylation (Fig. 5*A*), mainly observed at 8–14 min post-treatment. Similar data were observed in five independent experiments. Increased expression of CRMP2-pTyr-479 was concomitant with the decrease of CRMP2-Thr-509/514 as observed in Fig. 3*A*. This suggested a relationship between the phosphorylated Thr-509/514 and Tyr-479 sites. This hypothesis was evaluated by blocking GSK-3β activity using a cell-permeable peptide inhibitor (L803-mts, Calbiochem, 20 and 40 mM, 4 h). For this purpose we used a virus-infected T-cell line (C91PL) that constitutively expressed CRMP2-pTyr-479, possibly due to chronic activation. As expected, GSK-3β blockade resulted in the decrease in CRMP2-pThr-509/514. In parallel, CRMP2-pTyr-479 increased, validating our hypothesis (supplemental Fig. S2). Immunoblotting using antibody directed against a phospho-Yes1-Y537 peptide revealed the constitutive presence of p-Yes in the Jurkat T-cells, which was not significantly modified by CXCL12 treatment. This indicated that CRMP2-Tyr-479 phosphorylation by Yes under CXCL12 signaling might occur in Jurkat T-cells but mainly depended on site accessibility to this kinase.

Immunofluorescence was then performed on Jurkat cells treated with CXCL12 (15 min) using antibodies against the phosphorylated and non-phosphorylated CRMP2 forms. Staining for CRMP2-pTyr-479 was mainly with a polarized distribution in T lymphocytes (Fig. 5*B*).

TABLE 1

Identification of SH3 protein-CRMP2 interaction

CRMP2-His recombinant protein was incubated with a membrane spotted in duplicate with SH3 domains of 38 proteins (TranSignal™ SH3 Domain array I, Panomics) according to the manufacturer's instructions. Anti-His antibody revealed the association of CRMP2 with multiple SH3 domains, including those of some tyrosine kinase proteins. Spot intensities (− to +++) indicated the binding affinity of SH3 domains to the ligand CRMP2 and revealed Yes as a potent tyrosine kinase candidate for CRMP2.

		Strength of interaction with CRMP2
Tyrosine kinase proteins		
Yes1	Yamaguchi sarcoma virus oncogene homolog 1	++
Abl	Abelson tyrosine kinase	+
BLK	B-lymphocyte specific protein tyrosine kinase	+
LCK	Human T-lymphocyte specific protein tyrosine kinase	−
FYN	Proto-oncogene tyrosine protein kinase	−
BTK	Bruton tyrosine kinase	−
c-Src	Cellular rous sarcoma virus oncogene homolog 1	−
Hck	Hemopoietic cell kinase	−
TXK	Tyrosine-protein kinase TXK	−
Itk	Interleukin-2-inducible T-cell kinase	−
Non-kinase proteins		
PLCγ	Phospholipase C gamma-1	+++
VAV1	Vav proto-oncogen SH2 domain 1	++
PI3β	Phosphoinositide-3-kinase p85 regulatory β subunit	++
ITSN-D1	Intersectin, SH3 domain #1	+

Co-localization with vimentin showed that, compared with the CRMP2 forms recognized by the anti-pep4 and anti-C-ter antibodies, which were either co-distributed (*orange* as merged staining) or not (*green* staining) with vimentin, respectively, the phosphorylated CRMP2-Tyr-479 was mainly colocalized with vimentin at the trailing pole (Fig. 5*B*, *arrows*). Taken together, these results identified a new form of phosphorylated CRMP2 that was modulated by CXCL12 signaling, colocalized with cytoskeletal elements and could be targeted by the Src-family kinase Yes.

CRMP2-Tyr-479 Phosphorylation Is Involved in Chemokine-induced Polarization and Migration of T Cells—To assess the functional significance of CRMP2 phosphorylation on Tyr-479, we engineered the mutation Y479F on the full-length CRMP2 sequence. The effect of Tyr-479 phosphorylation impairment on T-cell polarization was then analyzed in Jurkat T-cells transiently transfected with FLAG-tagged CRMP2-wt and CRMP2-Y479F mutant. Twenty-four hours after transfection, T-cells were allowed to adhere onto collagen-I-coated slides, then treated with CXCL12 and examined by fluorescence microscopy. Polarization of CRMP2 in transfected T-cells, as visualized by FLAG-positive immunostaining (Fig. 6, *A*, *D*, *G*, and *J*), was examined based on vimentin network localization (Fig. 6, *C*, *F*, *I*, and *L*, *orange* as merge staining). This allowed us to evaluate the polarization of FLAG positive T-cells transfected either with CRMP2-wt or CRMP2-Y479F (expressed as a percentage of all transfected cells). The un-treated Jurkat T-cell population transfected with CRMP2-wt displayed ~28% spontaneously polarized cells, but this clearly decreased in T-cells transfected with the CRMP2-Y479F mutant (Fig. 6, *graph*). Following CXCL12 treatment, vimentin was quickly redistributed to the uropod in CRMP2-wt transfected T-cells (Fig. 6, *H* and *I*). In contrast, CRMP2-Y479F-transfected cells were clearly less polarized (Fig. 6, *K*, *L*, and *graph*). In addition, the increase in the number of polarized cells following CXCL12 treatment was lower in Jurkat T-cells transfected with CRMP2-Y479F than with CRMP2-wt (31% *versus* 42%, respectively) (Fig. 6, *graph*), thus confirming the impact of Tyr-479 phosphorylation on T-cell polarization. These results clearly showed the role of CRMP2-Tyr-479 phosphorylation in T lymphocyte polarization.

As T-cell polarization is a prerequisite for migration, we further evaluated the influence of Tyr-479 phosphorylation on T-cell migration. Thus, we first assessed the ability of transfected Jurkat T-cells to migrate toward CXCL12, by performing a transmigration assay in Transwell chambers. As shown in Fig. 7*A*, the rate of migration of CRMP2-Y479F-transfected cells was drastically reduced compared with those with CRMP2-wt and control cells (empty vector). Beyond T-cell transmigration that is necessary to traverse blood vessels, migration within invaded tissue is also a key point, especially within the central nervous system where CXCL12 and its cognate receptor are constitutively expressed. We therefore examined whether Tyr-479 phosphorylation had an influence on T-cell migration within neural tissue, using mouse hippocampal organotypic culture. Transfected Jurkat T-cells (40–50% transfection efficiency) were stained with the vital dye carboxyfluorescein succinimidyl ester to easily visualize them both on and in neural tissue (Fig. 7*B*). Cells were then spotted close to brain slices and were counted after 18-h incubation. CRMP2-Y479F-transfected cells displayed a reduced ability to travel on neural tissue compared with wild type-transfected cells. These results demonstrated the role of CRMP2-Tyr-479 phosphorylation in the process of T-cell migration within neural tissue.

DISCUSSION

To date, CRMP2 has essentially been known to specify neuronal polarity and promote axon elongation and branching in response to semaphorin by regulating microtubule assembly, reorganizing actin filaments and protein trafficking (22, 23). We recently showed that CRMP2 is expressed efficiently in T lymphocytes and demonstrated that these cells need CRMP2 to establish a polarized morphology and to engage in subsequent chemokine-directed migration (9), defining CRMP2 as a major player in cell polarity and motility within a larger field than just the nervous system. The present study undoubtedly establishes a link between CXCL12/CXCR4 signaling and CRMP2 in T lymphocytes.

CRMP2 Functions in Chemokine Signaling—Similar to other chemokines, CXCL12, when binding to its receptor CXCR4, activates a series of downstream signaling pathways, including heterotrimeric G-proteins, the Src family tyrosine kinases, and phosphoinositide 3-kinase, leading to cell polarization (24). The present observations prompted us to propose CRMP2 as part of this uropod signaling pathway. First, we showed that T lymphocytes treated with CXCL12 induced a re-localization of CRMP2 to the uropod of polarizing T-cells, a feature impaired by treatment with the CXCR4 antagonist AMD3100. This chemokine-induced change in intracellular distribution paralleled a modification of CRMP2 phosphorylation, together with an

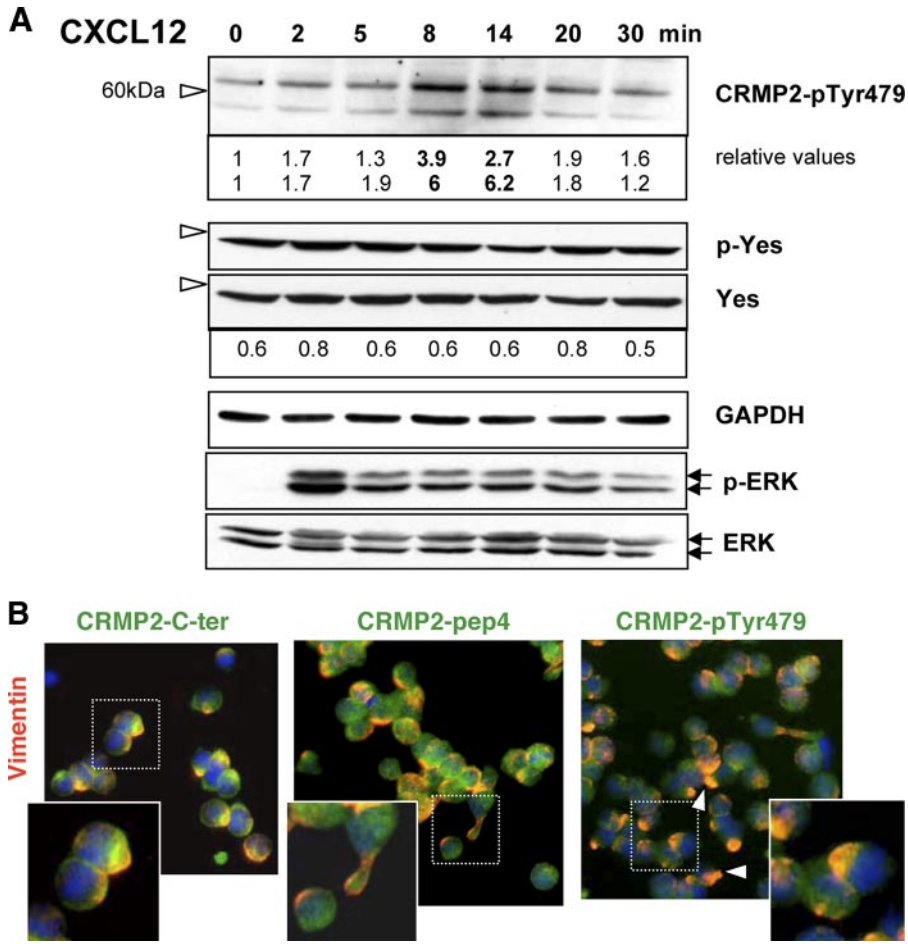

FIGURE 5. **CRMP2-pTyr-479 is enhanced and polarized in T-cells under CXCL12 treatment.** *A*, detection of CRMP2 phosphorylated on Tyr-479 in Jurkat cells with our polyclonal antibody raised against a peptide comprising the phosphorylated Tyr-479 residue. Western blotting revealed CRMP2-pTyr-479 in full-length and cleaved forms, which increased at 8–14 min following CXCL12 treatment (see relative values). Blotting against phospho-Yes1-Y537 revealed the constitutively active forms of Yes. *B*, co-immunodetection of vimentin (*red*) and CRMP2 (*green*) in Jurkat cells treated with CXCL12 (100 ng/ml, 15 min) using anti-CRMP2-pep4 and -C-ter antibodies and against CRMP2-pTyr-479. *Orange spots* (*merged color*) represent co-localization of CRMP2 forms and intermediate filament vimentin at uropod.

increased ability to bind cytoskeletal components. In addition, several SH3-binding proteins we identified as potential molecular partners of CRMP2 belong to the signaling cascade downstream of CXCR4. Notably, the association of CRMP2 with Vav-1, a guanine exchange factor with a pivotal role in migratory signal transmission through CXCR4 (25), suggests that CRMP2 is involved in recruitment at the uropod of signaling intermediates that transmit the chemotactic signal for cytoskeletal re-organization.

CRMP2 Is Involved in Cytoskeletal Re-organization under Chemokine Signaling—Similar to its crucial role as a regulator of cytoskeletal assembly in neural cells in response to semaphorin (16, 26, 27), CRMP2 is probably involved in the regulation of lymphocyte polarity in response to chemokine. We showed that CXCL12 enhanced CRMP2 recruitment on cytoskeletal elements, notably on vimentin, a molecule known to rapidly collapse into an aggregate within the uropod under chemokine signaling (28). This supports the idea of CRMP2 involvement in the maintenance and modulation of chemokine-induced T lymphocyte polarity and migration. As a potent molecular partner of actin, tubulin, kinesin-1, and of the endocytic proteins numb and intersectin (29, 30), CRMP2 could contribute to the dynamic reorientation of critical surface receptors/signaling proteins, selective vesicular traffic, and contraction/retraction from the front to the back required for cell movement, all orchestrated by the polarized actomyosin and microtubule cytoskeletons (review in Ref. 17).

CRMP2 Is Differentially Phosphorylated under CXCL12 Signaling—The exact implication of CRMP2 in chemokine-directed T-cell polarization and motility remains to be determined. However this certainly involves subtle changes in the CRMP2 phosphorylation state, because sequential phosphorylation near the C terminus by several serine/threonine kinases has been shown to be crucial for CRMP2 function in neural cells (18, 31). Briefly, Rho-kinase phosphorylates CRMP2 at Thr-555 under ephrin-A5 and myelin-associated glycoprotein signaling (32, 33), whereas Cdk5 phosphorylates CRMP2 at Ser-522 in response to Sema3A, priming the protein for subsequent phosphorylation by GSK-3β Thr-509 and Thr-514 (34). All these post-translational modifications result in a reduced affinity of CRMP2 for tubulin, leading to growth cone collapse and the inhibition of neurite outgrowth. Similar to what has been observed in neural cells, we found that CRMP2 was phosphorylated at Ser-522 and Thr-509/514 residues in resting T lymphocytes. CXCL12 differentially modulated CRMP2 phosphorylation at those sites, inducing a rapid de-phosphorylation at the GSK-3 target residue Thr-509/514, whereas phosphorylation of the Cdk5 site, Ser-522, remained relatively stable. Interestingly, Cdk5 and GSK-3β kinase activity paralleled these phosphorylation states. The major difference in the stability of phosphorylated Ser-522 and Thr-509/514 sites, recently reported in neural cells (35), could further explain the differential modulation of CRMP2 phosphorylation observed in T lymphocytes in response to chemokine. Indeed, these authors showed that protein phosphatase-1 rapidly de-phosphorylated CRMP2 at Thr-509/514 upon GSK-3 inhibition, whereas the Cdk5 site Ser-522 remained resistant to phosphatase treatment. In neural cells stimulated by insulin-like growth factor-1, brain-derived neurotrophic factor, and neurotrophin-3, GSK-3 inhibition and phosphatase-1 activity on CRMP2 promote CRMP2 de-phosphorylation, supporting microtubule assembly and axon outgrowth (31, 34). Accordingly, our present data suggest CXCL12

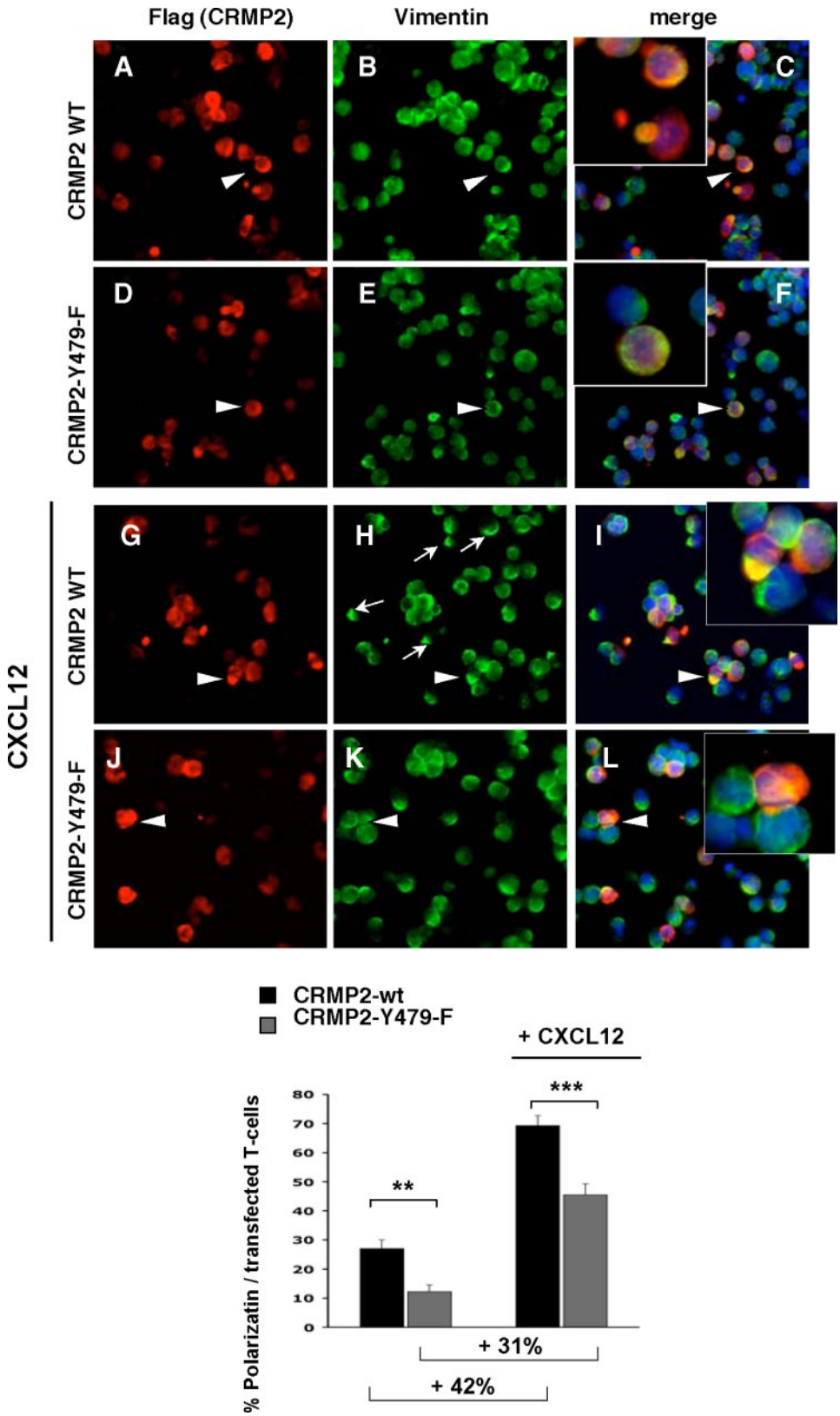

FIGURE 6. **CRMP2-Tyr-479 is involved in the chemokine-induced polarization of T-cells.** Jurkat cells were transfected with either CRMP2flag-wt (*A–C* and *G–I*) or CRMP2flag-Y479F mutant (*D–F* and *J–L*), allowed to adhere to collagen I-coated slides then treated with CXCL12 (*G–L*, 100 ng/ml). Polarization of transfected T-cells was visualized by co-detection of FLAG and vimentin. The quantification of polarized cells, expressed as percentages of all transfected cells, is shown graphically. Mutation of the tyrosine residue (CRMP2-Y479F mutant) specifically reduced spontaneous and chemokine-induced polarization (*graphical representation*).

as a further regulator of CRMP2 phosphorylation at the GSK-3 target site.

Another novelty of our work is the identification of a new phosphorylation site, Tyr-479, located at the C terminus near a putative SH3-binding motif. We showed that Yes, a non-receptor tyrosine kinase of the Src family, has the ability to phosphorylate CRMP2. This feature was compatible with the demonstration of Yes binding to CRMP2 through its SH3-domain. It is worth noting that CRMP2 showed the ability to bind Yes but not Fyn, Hck, Lck, Src, and Blk, which belong to the same kinase family. In fact, although Src family members share significant sequence and structural homology, these have been shown to serve not only redundant but also distinct functions (36). Phosphorylation of CRMP2-Tyr-479 by Yes kinase under chemokine signaling is conceivable, at least in Jurkat cells as they constitutively expressed the active Yes phosphorylated form and CRMP2-pTyr-479 level expression was noticeably enhanced following CXCL12 treatment.

The role of phosphorylation at Tyr-479 in functionally controlling CRMP2 under CXCL12 signaling was clear, because mutation of Tyr-479 profoundly altered CXCL12-induced polarization and greatly reduced the transmigration rate of T-cells and their ability to navigate *ex vivo* on neural tissue. It is therefore likely that phosphorylated CRMP2 forms recruited at the uropod, notably CRMP2-pTyr-479, would be included in the signalosome formed under CXCR4 activation. Intriguingly, CRMP2-pTyr-479 later appeared in chemokine-treated lymphocytes. One can propose several explanations for this. Accessibility to the tyrosine kinase site could be a limiting factor. We observed that Tyr-479 was not exposed on the surface of the CRMP2 molecule and probably required structural changes to become accessible to SH3-bearing molecular partners such as Yes. In fact, phosphorylation at this tyrosine site appeared when

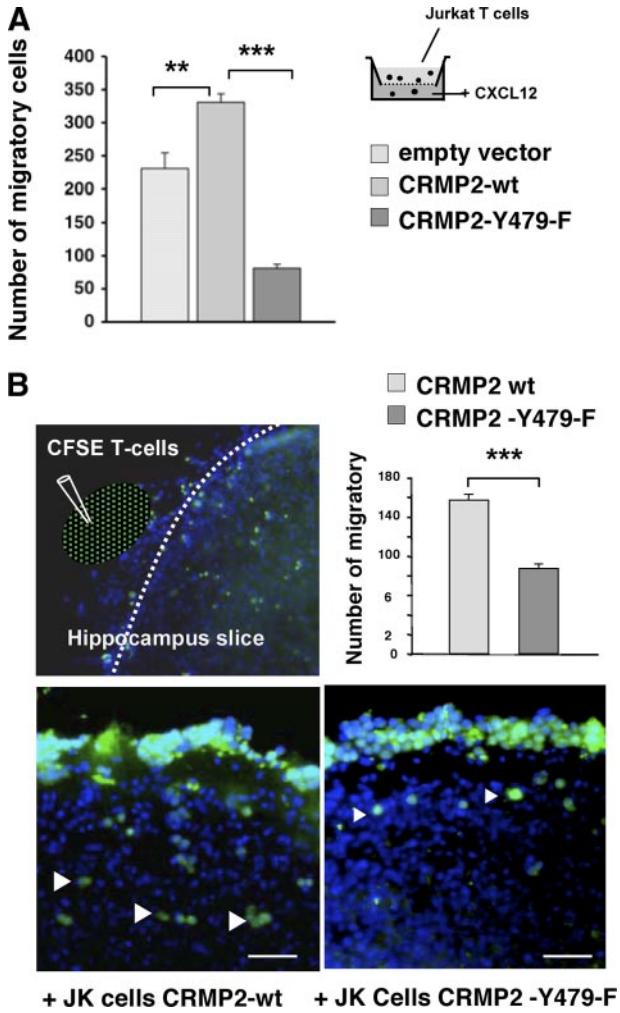

FIGURE 7. **Mutation of CRMP2-Tyr-479 resulted in reduced T lymphocyte migratory rates.** *A*, Jurkat cells transfected with either FLAG vector, CRMP2FLAG-wt or CRMP2FLAG-Y479F plasmids were examined for transmigration toward CXCL12 in Transwell chambers. Mutation of the tyrosine residue specifically reduced the migratory rate (*graphical representation*). *B*, for migration analysis on neural tissue, transfected Jurkat cells were stained with the vital dye carboxyfluorescein succinimidyl ester then spotted close to hippocampal organotypic slices and examined for migration using fluorescence microscope (*green color*). Counterstaining with DAPI visualized neural cell nuclei (*blue color*). Mutation of the tyrosine residue (CRMP2-Y479F) specifically reduced the ability of T-cells to navigate on neural tissue, as shown by quantification of migrating cells (*graphical representation*).

phosphorylation of the GSK-3 target (Thr-509/514) was no longer detectable. Furthermore, blockade of GSK-3β activity significantly reduced the pThr-509/514 form but increased pTyr-479. Thus, de-phosphorylation at Thr-509/514 could alter the overall charge of the protein sequence in the vicinity of Tyr-479, thus enhance the stability of phosphorylation at that site, in a manner similar to that for the Ser-522 site (35).

The Association of CRMP2 with CXCL12 Signaling Has Functional Significance—Given the ubiquitous pairing of CRMP2 and CXCR4, the CXCR4/Src/GSK-3/CRMP2 pathway described here might have consequences in several physiological and pathological situations. In the central nervous system, CXCL12 functions in localizing immune cells to the perivascular space, thereby limiting the parenchymal infiltration of autoreactive T-cells. However in patients with neuroinflammatory diseases, including multiple sclerosis, CXCL12 localization switches from a basolateral distribution toward the luminal and parenchymal sides of endothelial cells (37). Thus, CXCL12 accessibility at the blood-brain barrier and the elevated expression found in reactive astrocytes within active and chronic lesions in multiple sclerosis, probably promote T-cell infiltration in brain parenchyma (38). It is therefore tempting to speculate that CRMP2 is involved in the interplay between T lymphocytes, brain microvasculature, and neural cells. Indeed, we have detected elevated CRMP2 expression in activated T lymphocytes of patients suffering from neuroinflammatory diseases (9) and in the T-cells of mice developing either virus-induced neuroinflammation (12) or experimental autoimmune encephalitis (unpublished data). CRMP2 overexpression in peripheral T-cells was associated with high motility of selected human and mice T lymphocytes and with brain T-cell infiltration and high clinical scores in mouse models. Consequently, elevated chemokine signaling at the blood-brain barrier and CRMP2 activity in activated T-cell effectors might be required to orchestrate the infiltration of autoreactive T-cells in brain and thus disease progression in neuroinflammatory diseases.

It also appears that chemokines and their receptors have numerous roles to play in the developing and adult nervous systems (13). CRMP2 could participate in axon guidance and path finding regulated by the CXCL12/CXCR4 axis, because this has been recognized as decisive in regulating the migration of adult neural progenitors and axon projection of spinal motor neurons during development (39). In addition, a promising field of research has opened up in neuro-oncology as both CXCL12/CXCR4 and CRMP2 are up-regulated and hyperphosphorylated in brain tumors (40, 41).

In conclusion, we propose a novel regulation of CRMP2 activity that may be important for both the immune and nervous systems. Further studies should clarify the importance of the CXCR4/CRMP2 pathway either as a potential peripheral biomarker of neuroinflammation and tumor progression or as a target for further development of therapeutic strategies.

Acknowledgments—We thank Stéphan Menigoz for the illustration of the CRMP2 structure and Serge Nataf for critical reading of the manuscript.

REFERENCES

1. von Andrian, U. H., and Mempel, T. R. (2003) *Nat. Rev. Immunol.* **3,** 867–878
2. Bleul, C. C., Fuhlbrigge, R. C., Casasnovas, J. M., Aiuti, A., and Springer, T. A. (1996) *J. Exp. Med.* **184,** 1101–1109
3. Fredriksson, R., Lagerstrom, M. C., Lundin, L. G., and Schioth, H. B. (2003) *Mol. Pharmacol.* **63,** 1256–1272
4. Vicente-Manzanares, M., Viton, M., and Sanchez-Madrid, F. (2004) *Methods Mol. Biol.* **239,** 53–68
5. Serrador, J. M., Nieto, M., and Sanchez-Madrid, F. (1999) *Trends Cell Biol.* **9,** 228–233
6. Lataillade, J. J., Domenech, J., and Le Bousse-Kerdiles, M. C. (2004) *Eur. Cytokine Netw.* **15,** 177–188
7. Mellado, M., Rodriguez-Frade, J. M., Vila-Coro, A. J., Fernandez, S., Martin de Ana, A., Jones, D. R., Toran, J. L., and Martinez, A. C. (2001) *EMBO J.* **20,** 2497–2507
8. Patrussi, L., and Baldari, C. T. (2008) *Immunol. Lett.* **115,** 75–82
9. Vincent, P., Collette, Y., Marignier, R., Vuaillat, C., Rogemond, V., Davoust, N., Malcus, C., Cavagna, S., Gessain, A., Machuca-Gayet, I., Be-

lin, M. F., Quach, T., and Giraudon, P. (2005) *J. Immunol.* **175,** 7650–7660
10. Goshima, Y., Nakamura, F., Strittmatter, P., and Strittmatter, S. M. (1995) *Nature* **376,** 509–514
11. Charrier, E., Reibel, S., Rogemond, V., Aguera, M., Thomasset, N., and Honnorat, J. (2003) *Mol. Neurobiol.* **28,** 51–64
12. Vuaillat, C., Varrin-Doyer, M., Bernard, A., Sagardoy, I., Cavagna, S., Chounlamountri, I., Lafon, M., and Giraudon, P. (2008) *J. Neuroimmunol.* **193,** 38–51
13. Li, M., and Ransohoff, R. M. (2008) *Prog. Neurobiol.* **84,** 116–131
14. Rogemond, V., Auger, C., Giraudon, P., Becchi, M., Auvergnon, N., Belin, M. F., Honnorat, J., and Moradi-Ameli, M. (2008) *J. Biol. Chem.* **283,** 14751–14761
15. Stenmark, P., Ogg, D., Flodin, S., Flores, A., Kotenyova, T., Nyman, T., Nordlund, P., and Kursula, P. (2007) *J. Neurochem.* **101,** 906–917
16. Gu, Y., and Ihara, Y. (2000) *J. Biol. Chem.* **275,** 17917–17920
17. Krummel, M. F., and Macara, I. (2006) *Nat. Immunol.* **7,** 1143–1149
18. Uchida, Y., Ohshima, T., Sasaki, Y., Suzuki, H., Yanai, S., Yamashita, N., Nakamura, F., Takei, K., Ihara, Y., Mikoshiba, K., Kolattukudy, P., Honnorat, J., and Goshima, Y. (2005) *Genes Cells* **10,** 165–179
19. Martinez, J. C., and Serrano, L. (1999) *Nat. Struct. Biol.* **6,** 1010–1016
20. Quinn, C. C., Chen, E., Kinjo, T. G., Kelly, G., Bell, A. W., Elliott, R. C., McPherson, P. S., and Hockfield, S. (2003) *J. Neurosci.* **23,** 2815–2823
21. Buttner, B., Kannicht, C., Reutter, W., and Horstkorte, R. (2005) *Biochemistry* **44,** 6938–6947
22. Inagaki, N., Chihara, K., Arimura, N., Menager, C., Kawano, Y., Matsuo, N., Nishimura, T., Amano, M., and Kaibuchi, K. (2001) *Nat. Neurosci.* **4,** 781–782
23. Yoshimura, T., Arimura, N., and Kaibuchi, K. (2006) *Ann. N. Y. Acad. Sci.* **1086,** 116–125
24. Rot, A., and von Andrian, U. H. (2004) *Annu. Rev. Immunol.* **22,** 891–928
25. Vicente-Manzanares, M., Cruz-Adalia, A., Martin-Cofreces, N. B., Cabrero, J. R., Dosil, M., Alvarado-Sanchez, B., Bustelo, X. R., and Sanchez-Madrid, F. (2005) *Blood* **105,** 3026–3034
26. Fukata, Y., Itoh, T. J., Kimura, T., Menager, C., Nishimura, T., Shiromizu, T., Watanabe, H., Inagaki, N., Iwamatsu, A., Hotani, H., and Kaibuchi, K. (2002) *Nat. Cell Biol.* **4,** 583–591
27. Rosslenbroich, V., Dai, L., Baader, S. L., Noegel, A. A., Gieselmann, V., and Kappler, J. (2005) *Exp. Cell Res.* **310,** 434–444
28. Brown, M. J., Hallam, J. A., Colucci-Guyon, E., and Shaw, S. (2001) *J. Immunol.* **166,** 6640–6646
29. Kawano, Y., Yoshimura, T., Tsuboi, D., Kawabata, S., Kaneko-Kawano, T., Shirataki, H., Takenawa, T., and Kaibuchi, K. (2005) *Mol. Cell. Biol.* **25,** 9920–9935
30. Nishimura, T., Fukata, Y., Kato, K., Yamaguchi, T., Matsuura, Y., Kamiguchi, H., and Kaibuchi, K. (2003) *Nat. Cell Biol.* **5,** 819–826
31. Yoshimura, T., Kawano, Y., Arimura, N., Kawabata, S., Kikuchi, A., and Kaibuchi, K. (2005) *Cell* **120,** 137–149
32. Arimura, N., Menager, C., Kawano, Y., Yoshimura, T., Kawabata, S., Hattori, A., Fukata, Y., Amano, M., Goshima, Y., Inagaki, M., Morone, N., Usukura, J., and Kaibuchi, K. (2005) *Mol. Cell. Biol.* **25,** 9973–9984
33. Mimura, F., Yamagishi, S., Arimura, N., Fujitani, M., Kubo, T., Kaibuchi, K., and Yamashita, T. (2006) *J. Biol. Chem.* **281,** 15970–15979
34. Cole, A. R., Causeret, F., Yadirgi, G., Hastie, C. J., McLauchlan, H., McManus, E. J., Hernandez, F., Eickholt, B. J., Nikolic, M., and Sutherland, C. (2006) *J. Biol. Chem.* **281,** 16591–16598
35. Cole, A. R., Soutar, M. P., Rembutsu, M., van Aalten, L., Hastie, C. J., McLauchlan, H., Peggie, M., Balastik, M., Lu, K. P., and Sutherland, C. (2008) *J. Biol. Chem.* **283,** 18227–18237
36. Werdich, X. Q., and Penn, J. S. (2005) *Angiogenesis* **8,** 315–326
37. McCandless, E. E., Piccio, L., Woerner, B. M., Schmidt, R. E., Rubin, J. B., Cross, A. H., and Klein, R. S. (2008) *Am. J. Pathol.* **172,** 799–808
38. Calderon, T. M., Eugenin, E. A., Lopez, L., Kumar, S. S., Hesselgesser, J., Raine, C. S., and Berman, J. W. (2006) *J. Neuroimmunol.* **177,** 27–39
39. Lieberam, I., Agalliu, D., Nagasawa, T., Ericson, J., and Jessell, T. M. (2005) *Neuron* **47,** 667–679
40. Rubin, J. B., Kung, A. L., Klein, R. S., Chan, J. A., Sun, Y., Schmidt, K., Kieran, M. W., Luster, A. D., and Segal, R. A. (2003) *Proc. Natl. Acad. Sci. U. S. A.* **100,** 13513–13518
41. Tahimic, C. G., Tomimatsu, N., Nishigaki, R., Fukuhara, A., Toda, T., Kaibuchi, K., Shiota, G., Oshimura, M., and Kurimasa, A. (2006) *Biochem. Biophys. Res. Commun.* **340,** 1244–1250